

# The hierarchical reference theory as applied to square well fluids of variable range

Albert Reiner<sup>a)</sup> and Gerhard Kahl

*Institut für Theoretische Physik and Center for Computational Materials Science, Technische Universität Wien, Wiedner Hauptstraße 8–10, A-1040 Vienna, Austria*

(Received 30 January 2002; accepted 15 April 2002)

Continuing our investigation into the numerical properties of the *hierarchical reference theory*, we study the square well fluid of range  $\lambda$  from slightly above unity up to 3.6. After briefly touching upon the core condition and the related decoupling assumption necessary for numerical calculations, we shed some light on the way an inappropriate choice of the boundary condition imposed at high density may adversely affect the numerical results; we also discuss the problem of the partial differential equation becoming stiff for close-to-critical and subcritical temperatures. While agreement of the theory's predictions with simulational and purely theoretical studies of the square well system is generally satisfactory for  $\lambda \geq 2$ , the combination of stiffness and the closure chosen is found to render the critical point numerically inaccessible in the current formulation of the theory for most of the systems with narrower wells. The mechanism responsible for some deficiencies is illuminated at least partially and allows us to conclude that the specific difficulties encountered for square wells are not likely to resurface for continuous potentials. © 2002 American Institute of Physics. [DOI: 10.1063/1.1483258]

## I. INTRODUCTION

In a large part of the density–temperature plane, integral equation theories are a reliable tool for studying thermodynamic and structural properties of, among others, simple one-component fluids;<sup>1</sup> unfortunately, in the vicinity of a liquid–vapor critical point, integral equations are haunted by a host of difficulties, leading to a variety of shortcomings such as incorrect and nonmatching branches of the binodal, classical values at best for the critical exponents, or other deviations from the correct behavior at the critical singularity.<sup>2</sup> Asymptotically close to the critical point, on the other hand, renormalization group (RG) theory is the instrument of choice for describing the fluid; in general, however, RG approaches do not allow one to derive nonuniversal quantities from microscopic information only, i.e., from knowledge of the forces acting between the fluid's particles alone. One of the theories devised to bridge the conceptual gap between these complementary approaches is the *hierarchical reference theory* (HRT) first put forward by Parola, Reatto, and co-workers.<sup>2–13</sup> In this theory the introduction of a cutoff wave number  $Q$  inspired by momentum space RG theory and, for every value of  $Q$ , of a renormalized potential  $v^{(Q)}(r)$  means that only noncritical systems have to be considered at any stage of the calculation; consequently, integral equations may successfully be applied to every system with  $Q > 0$ , and critical behavior characterized by nonclassical critical exponents is recovered only in the limit  $Q \rightarrow 0$ .

While applicability of HRT to a number of interesting systems, ranging from a lattice gas or Ising model<sup>11</sup> to various one-component fluids<sup>6–8</sup> even including three-body interactions,<sup>13,14</sup> internal degrees of freedom,<sup>15</sup> or non-hard-

core reference systems,<sup>16</sup> was demonstrated early on, the main focus of research on HRT has since shifted to the richer phase behavior of binary systems.<sup>16–18</sup> Nevertheless, in light of HRT's high promise and low penetration into the liquid physics community, further study and critical assessment of this theory seem worthwhile, even and foremost in the case of simple one-component fluids: indeed, it is in this comparatively simple setting that we may gain important insight into the numerical side of the theory, and barring special mechanisms relevant to some specific model system only, any problems uncovered here must be expected to haunt more advanced applications of HRT, too. In our work we have found it convenient to restrict ourselves even further, implementing HRT in its usual formulation<sup>2,19,20</sup> for purely pairwise additive interactions *via* a potential  $v(r)$  obtained from the superposition of an infinitely repulsive hard sphere serving as reference system,  $v^{\text{ref}}(r) = v^{\text{hs}}(r)$ , and a predominantly attractive tail  $w(r)$ ,  $\tilde{w}(0) < 0$ . Here we have made use of the notation introduced previously:<sup>19</sup> superscripts always denote the system a quantity refers to [here, “ref” and “hs” for the reference system and hard spheres, respectively; similarly, “(Q)” for the system with cutoff  $Q$ ], and a tilde indicates Fourier transformation. In the present contribution we apply our recent reimplementation of the theory<sup>19</sup> to one of the simplest potentials exhibiting phase separation, viz., the square well potential  $v^{\text{sw}[-\epsilon, \lambda, \sigma]}$  (cf. Sec. III B of Ref. 19):

$$v^{\text{sw}[-\epsilon, \lambda, \sigma]}(r) = v^{\text{hs}[\sigma]}(r) + w^{\text{sw}[-\epsilon, \lambda, \sigma]}(r),$$

$$v^{\text{hs}[\sigma]}(r) = \begin{cases} +\infty, & r < \sigma \\ 0, & r > \sigma, \end{cases} \quad (1)$$

$$w^{\text{sw}[-\epsilon, \lambda, \sigma]}(r) = \begin{cases} -\epsilon, & r < \lambda \sigma \\ 0, & r > \lambda \sigma. \end{cases}$$

<sup>a)</sup>Electronic mail: areiner@tph.tuwien.ac.at

Considering density-independent potentials only and choosing the hard-core diameter  $\sigma$  and the well's depth  $\epsilon$  as units of length and energy, respectively, the attractive well's range  $\lambda$  is the sole remaining parameter; in this article we will study values of  $\lambda$  from slightly above unity up to 3.6.

With just one parameter, viz.,  $\lambda$ , to vary, square wells obviously make for a convenient test case of HRT and, indeed, of liquid state theories in general; consequently, a great many simulational and theoretical efforts have been directed at this system, and studies of its phase behavior abound.<sup>21–33</sup> But square wells are also of interest in their own right, serving as—albeit somewhat crude—models of a wide variety of physical systems including, e.g., <sup>3</sup>He, Ne, Ar, H<sub>2</sub>, CO<sub>2</sub>, CH<sub>4</sub>, C<sub>2</sub>H<sub>6</sub>, *n*-pentane, and *n*-butane,<sup>33–35</sup> while current interest in this potential derives mainly from the finding that square wells capture the essential features of the interactions found in colloidal systems.<sup>36–40</sup> Yet another motivation for this first application of HRT to square wells comes from a recent, very accurate simulation study<sup>31</sup> confirming and quantifying the presence in the system with  $\lambda = 1.5$  of the Yang–Yang (YY) anomaly expected and experimentally found for asymmetric fluids.<sup>41,42</sup>

Due to the extensive amount of data available in the literature the more recent of which will shortly be presented later on, and in view of some of the limitations of HRT in its current formulation we cannot expect to gain new insight into the system at hand with a level of precision comparable to that of the more sophisticated simulation schemes. Instead, in the present contribution our focus of interest lies on some aspects of HRT's numerical side, specifically on those that are sensitive to the potential's range: indeed, as stated already in Ref. 19, for a potential as pronouncedly short-ranged as square wells some of the numerical problems should show up much more prominently than in other systems like, e.g., the hard-core Yukawa fluid previously considered<sup>19</sup> where they are, of course, in principle still present but do not manifest themselves as clearly.

In accordance with the preceding remarks, another reason why application of HRT to square wells might be worthwhile lies in the closure underlying seemingly all applications so far of HRT to simple one-component fluids with hard-sphere reference part: As the usual formulation of HRT in these cases relies on an *ansatz* for the two-particle direct correlation function  $c_2(r)$  very much in the spirit of Stell's *lowest-order  $\gamma$ -ordered approximation*<sup>43,44</sup> (LOGA) or the equivalent *optimized random-phase approximation*<sup>45</sup> (ORPA) by Andersen and Chandler, the direct correlation function can never extend to larger  $r$  values than the potential  $v(r)$  itself. In particular, for the square well potential  $v^{\text{sw}[-\epsilon, \lambda, \sigma]}(r)$  we necessarily have  $c_2(r) = 0$  for  $r > \lambda \sigma$  so that all moments of  $c_2(r)$ , i.e.,  $\int_{\mathbb{R}^3} d^3r c_2(r) r^n$ ,  $n \geq 0$ , exist, which is obviously at variance with the correct behavior near the critical point;<sup>46</sup> furthermore, at intermediate  $Q$  the direct correlation function can hardly be considered satisfactory, especially<sup>19,20</sup> close to  $r = \lambda \sigma$ . While some earlier publications<sup>6,13,47</sup> already blamed unsatisfactory aspects of HRT results on this inadequacy of the closure, square wells should bring out related problems of HRT with the usual LOGA/ORPA-style closure much more clearly, and the nu-

merical procedure's response should provide us with a signature to be looked out for in other systems, too; also, even within the LOGA/ORPA-style approximation the implementation of the core condition *via* approximate ordinary differential equations (ODEs) for the relevant expansion coefficients easily shown to be inadequate for very short-ranged potentials<sup>20</sup> casts some doubt on the range of  $\lambda$  values amenable to an HRT treatment in the current formulation of the theory. Determination of the admissible  $\lambda$  range, on the other hand, is particularly interesting in light of Refs. 27 and 47 as well as in view of the global renormalization scheme<sup>32–35</sup> originally developed by White and co-workers as an extension of Wilson's phase-space cell method<sup>48</sup> to the liquid state; it is only by combining tests internal to the theory and comparison with data available by other means that we are able to answer this question.

In this contribution, after a sketchy presentation of the underlying theory itself (Sec. II) and the implementation used (Sec. III), in Sec. IV we turn to the results of applying HRT to square well systems of variable range. After a short summary of the critical point's location as obtained from simulation-based and other purely theoretical studies of square wells for various values of  $\lambda$  (Sec. IV A) we first look into the core condition's implementation, which provides us with a first hint regarding the range of  $\lambda$  values accessible to HRT in its current formulation and once more highlights the decoupling assumption's role (Sec. IV B). The latter is also implicated in the correct choice of the boundary condition imposed at high density as discussed, alongside the effect of its location in Sec. IV C. A particularly grave aspect of HRT's numerical side is the stiffness of the partial differential equation (PDE) for close-to-critical and subcritical temperatures (Sec. IV D), the vestiges of which are evident in the results obtained for quasicontinually varying  $\lambda$  as presented in Sec. IV E. A short summary of our findings and conclusions ends our contribution (Sec. V).

## II. THE THEORY

The definite resource on HRT is the review<sup>2</sup> by the theory's original authors, summarizing its formalism as developed in a series of earlier publications<sup>3–8</sup> so that we here present only an overview of the theory used and of its formulation, recapitulating some of our earlier findings;<sup>19</sup> the notation employed here of course coincides with that of our preceding contribution.<sup>19</sup>

As mentioned already in Sec. I, HRT's mainstay is the implementation of the suppression of long-wavelength fluctuations characteristic of RG methods by means of a renormalized potential  $v^{(Q)}$ . Thus, rather than directly going from a reference fluid the properties of which are assumed known to the fully interacting system, i.e., from pair potential  $v^{\text{ref}}(r)$  to  $v(r) = v^{\text{ref}}(r) + w(r)$ , HRT proceeds *via* a succession of rather artificial<sup>19</sup> intermediate potentials  $v^{(Q)}(r)$ : For every value of the cutoff wave number  $Q$ ,  $v^{(Q)}$  is given by

$$v^{(Q)}(r) = v^{\text{ref}}(r) + w^{(Q)}(r),$$

$$\tilde{w}^{(Q)}(k) = \begin{cases} \tilde{w}(k), & k > Q \\ 0, & k < Q \end{cases}$$

$$\bar{w}^{\text{sw}[-\epsilon,\lambda,\sigma]}(k) = -4\pi\epsilon \frac{\sin\lambda\sigma k - \lambda\sigma k \cos\lambda\sigma k}{k^3},$$

where the last line specializes to the square well potential of Eq. (1); obviously,  $v^{\text{ref}}$  and  $v$  are recovered in the limits  $Q \rightarrow \infty$  and  $Q \rightarrow 0$ ,

$$v^{(\infty)}(r) = v^{\text{ref}}(r) = v^{\text{hs}}(r), \quad v^{(0)}(r) = v(r) = v^{\text{sw}}(r),$$

allowing HRT to gradually turn on fluctuations of ever increasing wavelength by lowering  $Q$  from  $\infty$  to zero (numerically,<sup>19</sup> from  $Q_\infty$  to  $Q_0$ ); as mentioned before, criticality (together with nonclassical critical exponents) and phase separation (with isotherms rigorously flat in the two phase region) are obtained in the limit  $Q \rightarrow 0$ . In this procedure it is essential to maintain the differential picture implied by RG theory and to make sure that the transition from  $Q$  to infinitesimally smaller cutoff  $Q - dQ$  is continuous even in the limit  $Q \rightarrow 0$ . The latter requirement necessitates replacing the usual free energy  $A^{(Q)}$  and two-particle direct correlation function  $c_2^{(Q)}(r)$  of the hypothetical system with cutoff  $Q$  and potential  $v^{(Q)}(r)$ , the “ $Q$  system,” by suitably modified quantities, viz.,

$$\frac{\beta A^{(Q)}}{V} = \frac{\beta A^{(Q)}}{V} - \frac{\varrho^2}{2} [\bar{\phi}(0) - \bar{\phi}^{(Q)}(0)] + \frac{\varrho}{2} [\phi(0) - \phi^{(Q)}(0)],$$

$$C^{(Q)}(r) = c_2^{(Q)}(r) + \phi(r) - \phi^{(Q)}(r),$$

$$\phi = -\beta w, \quad \beta = 1/k_B T,$$

where  $\varrho$  is the number density of the system at hand; the higher-order correlation functions  $c_n^{(Q)}(r_1, \dots, r_n)$ ,  $n \geq 3$ , are free from such problems. [Note that all the direct correlation functions including  $C^{(Q)}(r)$  are taken to include the ideal gas terms.<sup>2]</sup>

With this set of quantities continuous even in the limit  $Q \rightarrow 0$ , viz.,  $A^{(Q)}$ ,  $C^{(Q)}$ , and the  $c_n^{(Q)}$ ,  $n \geq 3$ , HRT is derived as a nonterminating hierarchy of coupled ODEs at fixed density  $\varrho$ , calculating the properties of the  $Q$  system by treating the system at infinitesimally higher cutoff  $Q + dQ$  as a reference system; of these equations, usually only the evolution equation for  $A^{(Q)}$ , viz.,

$$\frac{d}{dQ} \left( \frac{\beta A^{(Q)}}{V} \right) = \frac{Q^2}{4\pi^2} \ln \left( 1 - \frac{\bar{\phi}(Q)}{\bar{c}^{(Q)}(Q)} \right), \quad (2)$$

as well as the important compressibility sum rule

$$\bar{c}^{(Q)}(0) = - \frac{\partial^2}{\partial \varrho^2} \left( \frac{\beta A^{(Q)}}{V} \right) \quad (3)$$

valid for any cutoff  $Q$  directly enter practical calculations.

When combined with a closure on the two-particle level, Eqs. (2) and (3) define a PDE in the  $(Q, \varrho)$  plane; it is this PDE that we will concern ourselves with in the remainder of this text. Said closure, reminiscent of LOGA/ORPA but adding one free parameter to allow imposing thermodynamic consistency as embodied in Eq. (3), is given, just as in our earlier contribution,<sup>19</sup> by

$$\begin{aligned} C^{(Q)}(r, \varrho) &= \phi(r, \varrho) + \gamma_0^{(Q)}(\varrho) u_0(r, \varrho) + \mathcal{K}^{(Q)}(r, \varrho), \\ \mathcal{K}^{(Q)}(r, \varrho) &= \mathcal{G}^{(Q)}(r, \varrho) + c_2^{\text{ref}}(r, \varrho), \\ \mathcal{G}^{(Q)}(r, \varrho) &= \sum_{n=1}^{\infty} \gamma_n^{(Q)}(\varrho) u_n(r, \varrho), \end{aligned} \quad (4)$$

where we have generalized to density-dependent potentials. The basis function  $u_0(r, \varrho)$  is chosen to coincide with<sup>20</sup>  $w(r, \varrho)/\bar{w}(0, \varrho)$ , and the higher basis functions  $u_n(r, \varrho)$ ,  $n \geq 1$ , vanish outside the core; for our specific choice of basis functions see Appendix B of Ref. 19. In order to ensure that both the core condition, i.e.,  $g(r, \varrho) = 0$  for  $r < \sigma(\varrho)$  where  $g(r, \varrho)$  is the pair distribution function, and sum rule (3) are met it is necessary to choose the correct set of expansion coefficients  $\gamma_n^{(Q)}(\varrho)$ ,  $n \geq 0$ , at every cutoff  $Q$  and for every density  $\varrho$ ; assuming their validity for  $Q = \infty$  and adopting the shorthand notations

$$\alpha^{(Q)}(\varrho) = \frac{\partial^3}{\partial Q \partial \varrho^2} \left( \frac{\beta A^{(Q)}}{V} \right),$$

$$\hat{\mathcal{I}}^{(Q)}[\psi(k, \varrho), \varrho] = \int_{\mathbb{R}^3} \frac{d^3k}{(2\pi)^3} \frac{\psi(k, \varrho)}{[\bar{c}_2^{(Q)}(k, \varrho)]^2}$$

(here,  $\psi$  is an arbitrary function of  $k$  and  $\varrho$ ), both relations can be combined to

$$\begin{aligned} &\sum_{n=1}^{\infty} \hat{\mathcal{I}}^{(Q)}[\bar{u}_j(k, \varrho) [\bar{u}_n(k, \varrho) - \bar{u}_0(k, \varrho) \bar{u}_n(0, \varrho)], \varrho] \frac{\partial \gamma_n^{(Q)}(\varrho)}{\partial Q} \\ &= \alpha^{(Q)}(\varrho) \hat{\mathcal{I}}^{(Q)}[\bar{u}_j(k, \varrho) \bar{u}_0(k, \varrho), \varrho] \\ &+ \frac{Q^2}{2\pi^2} \frac{\bar{\phi}(Q, \varrho) \bar{u}_j(Q, \varrho)}{\bar{c}^{(Q)}(Q, \varrho) [\bar{c}^{(Q)}(Q, \varrho) - \bar{\phi}(Q, \varrho)]}, \quad j \geq 1; \end{aligned} \quad (5)$$

this set of equations must, of course, be truncated to a finite number  $1 + N_{\text{cc}}$  of basis functions, and it is also necessary to neglect nonlocal contributions to  $\partial \hat{\mathcal{I}}^{(Q)}[\psi(k, \varrho), \varrho] / \partial Q$  to allow convenient evaluation at arbitrary  $Q$ . Both of these approximations have been discussed at length in our previous contribution,<sup>19</sup> and while the value of  $N_{\text{cc}}$  was found to strongly influence the quality of the results obtained, determination of the  $\gamma_n^{(Q)}(\varrho)$  from Eq. (5) and said approximation for the slowly converging  $\hat{\mathcal{I}}$  integrals'  $Q$  dependence leads to systematic deficiencies at small  $r$  in  $g(r)$  as determined from the Ornstein–Zernike relation.

Unfortunately, for numerical reasons<sup>19</sup> it is necessary to also adopt the so-called decoupling assumption,<sup>8</sup> viz.,  $\alpha^{(Q)}(\varrho) = 0$ ; as can easily be seen, this is not only mathematically incompatible with thermodynamic consistency but even suffices to decouple the PDE implied by Eqs. (2) and (3) to a set of unrelated ODEs at fixed density only lacking thermodynamic consistency and thus unable to predict clear phase boundaries.<sup>19</sup> Furthermore, we cannot rule out that decoupling may have a significant influence on the solution generated,<sup>19</sup> which is particularly troublesome as the much longer range of  $u_0(r) \propto \phi(r)$  when compared with the other basis functions was originally invoked as justification for setting  $\alpha^{(Q)}(\varrho) = 0$ . For square wells, this assumption is certainly even less justified than for the rather long-ranged

hard-core Yukawa system ( $z=1.8/\sigma$ ) considered in Ref. 19.

Returning to the PDE, for the numerical implementation's benefit we, too, adopted a reformulation in terms of an auxiliary function  $f(Q, \varrho)$  simply related to the modified free energy's derivative with respect to  $Q$ . The details of the procedure leading to a PDE of the form

$$\begin{aligned} \frac{\partial}{\partial Q} f(Q, \varrho) &= d_{00}[f, Q, \varrho] + d_{01}[f, Q, \varrho] \frac{\partial}{\partial \varrho} f(Q, \varrho) \\ &\quad + d_{02}[f, Q, \varrho] \frac{\partial^2}{\partial \varrho^2} f(Q, \varrho), \\ f(Q, \varrho) \tilde{u}_0^2(Q, \varrho) &= \ln \left( 1 - \frac{\tilde{\phi}(Q, \varrho)}{\tilde{c}^{(Q)}(Q, \varrho)} \right) + \frac{\tilde{\phi}(Q, \varrho)}{\tilde{\kappa}^{(Q)}(Q, \varrho)}, \end{aligned} \quad (6)$$

and the coefficient functions  $d_{0i}$  themselves can be found in Appendix A of Ref. 19, q.v. Ref. 20.

The above formulation (6) of the problem, of course still coupled to the ODEs implementing the core condition, obviously has to be amended by initial and boundary conditions. While the former easily follow from  $\gamma_n^{(Q_\infty)}=0$ ,  $n \geq 0$  [which is sufficient to also determine  $f(Q_\infty, \varrho)$ ], choice of appropriate boundary conditions is slightly more complicated. If, as is the case in most of the calculations reported here (see below for exceptions), the low-density boundary is located at  $\varrho_{\min}=0$ , we can make use of the divergence of the ideal gas term  $-1/\varrho$  in  $\tilde{c}_2^{\text{ref}}$  to derive not only  $f(Q, 0)=0$  but also  $\partial f(Q, 0)/\partial \varrho=0$ , which alone is, in principle, sufficient to uniquely determine the solution up to arbitrarily high density. For computational reasons, however, it is preferable to instead only impose vanishing  $f$  at  $\varrho_{\min}$  and to supply an approximate condition for calculating  $f$  at  $\varrho_{\max}$ . Among the candidates for the constraint to be imposed upon the solution at  $\varrho_{\max}$  in addition to the core condition there are two we should mention here: Starting with Ref. 7, the so-called ORPA condition, viz.,  $\gamma_0^{(Q)}(\varrho_{\max})=0$ , has been used extensively. It should, however, be noted that this condition is incompatible with both thermodynamic consistency and the decoupling assumption.<sup>19</sup> An alternative first considered in our previous report<sup>19</sup> is the decoupling assumption  $\alpha^{(Q)}(\varrho_{\max})=0$  itself; of course, this condition is still incompatible with the compressibility sum rule (3) but this is less of a problem at a boundary where partial derivatives with respect to  $\varrho$  cannot be evaluated anyway. Another option (not pursued in this contribution) is to give up the core condition altogether, retaining only the lowest basis function  $u_0$  in the closure (4) and thus effectively replacing Eq. (5) by Eq. (3); this has the added advantage of mathematical consistency while still retaining the structure of a PDE so important for obtaining clear phase boundaries,<sup>19</sup> see above.

It is one of HRT's main achievements to allow calculating a fluid's binodal (coinciding with the spinodal in three dimensions<sup>12</sup>) without resorting to Maxwell constructions,<sup>12</sup> for subcritical temperatures yielding isotherms rigorously flat in density intervals the boundaries of which are readily identified with the coexisting densities  $\varrho_v$  and  $\varrho_l$ . Thus, as the isothermal compressibility  $\kappa_T$  of the fully interacting system, readily found to be proportional to  $\exp[f - (\tilde{\phi}(0)/\tilde{\kappa}^{(0)})] - 1$

(cf. Appendix A of Ref. 19), diverges in the two-phase region, so must the auxiliary function  $f(Q, \varrho)$  in the limit  $Q \rightarrow 0$ . As a direct consequence, the transition from the modified free energy  $\mathcal{A}^{(Q)}(\varrho)$  to  $f(Q, \varrho)$  is not only computationally convenient but also allows us to follow the isothermal compressibility's buildup much more easily; even more importantly, a simple analysis<sup>19,20</sup> of the behavior of the PDE's coefficients for large  $f(Q, \varrho)$  readily characterizes the PDE as stiff: for any density  $\varrho \in [\varrho_v, \varrho_l]$  and close to  $Q=0$ , the true solution  $f(Q, \varrho)$  oscillates rapidly on a  $Q$  scale of the order of  $\exp(-f)$ , with both an upper bound on the oscillations' amplitudes and  $f$ 's average slope growing like  $1/Q$ —needless to say that this behavior cannot be reproduced numerically (see Sec. IV D; q.v. Ref. 19). Note, however, that it is not an artifact of the rewriting of the PDE in the form (6) but rather a problem inherent to HRT itself in a formulation based upon Eq. (4).<sup>20</sup>

### III. NUMERICAL PROCEDURE

The numerical study of HRT for square well systems of varying range parameter  $\lambda$  in Sec. IV has only become feasible due to our recent reimplementations<sup>49</sup> of this theory, discussed at length in Refs. 19 and 20; we will make use of results obtained with this program exclusively. From a practical point of view, our software provides a means of solving a finite-difference approximation to the PDE (6) in an iterated full-approximation scheme, imposing boundary conditions at densities  $\varrho_{\min}$  and  $\varrho_{\max}$  as well as initial conditions at  $Q=Q_\infty$ , generating a solution for  $Q$  as low as  $Q_0$  while ensuring numerical soundness of every step by employing a number of criteria. The pivotal parameter governing all of the numerics is a small quantity denoted  $\epsilon_\#$  characteristic of the maximum admissible relative error introduced in a single step in the  $-Q$  direction; due to the paramount importance of derivatives with respect to  $\varrho$ ,  $\epsilon_\#$  is strictly related to the coarseness of the density grid.

The only exception to the general strategy of ensuring a numerical quality of  $\epsilon_\#$  at every step in the calculation is the choice of step sizes  $\Delta Q$  in the  $-Q$  direction, at least for subcritical and close-to-critical temperatures: indeed, in that part of the  $(Q, \varrho)$  plane where the divergence of the isothermal compressibility builds up, the PDE's stiffness (see above) renders fixed-precision arithmetic and relative errors bounded by  $\epsilon_\#$  incompatible. Consequently, for the calculations reported below we resort to step sizes  $\Delta Q$  predetermined in a way analogous to that employed in earlier applications;<sup>6,19</sup> still, monitoring and assessing suitable components of the solution vector in terms of  $\epsilon_\#$  as described in Sec. III E of Ref. 19 may yield a wealth of information on the numerical process and its evolution.

Most of the calculations reported here have been performed on an equispaced density grid of  $N_\varrho=100$  density intervals spanning the range from  $\varrho_{\min}=0$  to  $\varrho_{\max}=1/\sigma^3$ , corresponding to a value of  $\epsilon_\#=10^{-2}$ ;  $N_{cc}$  was usually set to 7; and the predetermined step sizes started from  $\Delta Q = -10^{-2}/\sigma$  at  $Q_\infty=80/\sigma$ , plunging to a mere  $-5 \times 10^{-6}/\sigma$  when approaching  $Q_0=10^{-4}/\sigma$ . When locat-

ing the binodal via the divergence of the isothermal compressibility  $\kappa_T$  we did not require an actual overflow to occur but instead looked for a  $\kappa_T$  ratio at neighboring densities exceeding  $10^4$ , which is a rather reliable indicator for the binodal's location as  $\kappa_T$  typically jumps by far less than two or by at least some twenty orders of magnitude within one  $\Delta\varrho$ ; the reported values for  $\varrho_v$  and  $\varrho_l$  are the midpoints of the density intervals so found. In principle this allows us to locate the coexisting densities and the critical temperature and density to arbitrary precision, even though the computational cost rises sharply with falling  $\epsilon_{\#}$ .

#### IV. APPLICATION TO SQUARE WELLS

As mentioned before, much of the motivation for applying HRT in the formulation outlined in Sec. II to the simple square well model potential is based upon various observations indicating possible limitations of this approximate formulation of HRT for short-ranged potentials. A case in point is the recent work of Caccamo *et al.*<sup>47</sup> entirely devoted to several thermodynamically consistent theories' ability to deal with narrow hard-core Yukawa systems; sure enough, in the case of HRT the shortcomings of the LOGA/ORPA-style closure (4) and, presumably, of the accompanying decoupling assumption underlying the core condition's implementation via Eq. (5) were manifest already in Refs. 6 and 13 and recently confirmed by us,<sup>19</sup> q.v. Ref. 20.

Of course, any of the problems discussed below only relate to HRT when implemented along the lines of Secs. II and III and not to HRT proper; however, for reasons discussed in Ref. 19, alternative formulations almost certainly render the numerics far more demanding and open up a whole new suite of problems regarding the numerical implementation's soundness, especially when performing Fourier transformations of cutoff-affected functions.<sup>20</sup>

In the following subsections we will complement the discussion of Ref. 19 by further investigation into the numerical nature of HRT; before that, however, it seems pertinent to reiterate some of the points raised in that publication as far as they concern the reasoning to be put forward in the following. In particular, according to Sec. IV of Ref. 19, for the numerical results to be meaningful the coexisting densities  $\varrho_v$  and  $\varrho_l$  must maintain a separation of at least several density grid spacings  $\Delta\varrho$  from the boundaries at  $\varrho_{\min}$  and  $\varrho_{\max}$ ; consequently,  $\beta$  should never exceed some maximum value,  $\beta < \beta_{\max}$ , and for the systems considered here and in Ref. 19 and for the typical choices for  $\varrho_{\min}$  and  $\varrho_{\max}$  the binodal's proximity to the low density boundary renders  $\beta_{\max}$  largely density grid and  $\epsilon_{\#}$  independent.

Not to be confused with  $\beta_{\max}$  is the lowest temperature  $k_B/\beta_{\max,\#}$  numerically accessible to the program with predetermined step sizes: this is the temperature below which the program of Sec. III never reaches  $Q \approx Q_0$  or produces abnormal results; note that  $\beta_{\max,\#}$  may be larger or smaller than  $\beta_{\max}$ , depending on the chosen combination of physical potential, approximations in the formulation used (the boundary conditions in particular), and the choice of parameters affecting the numerical work.

Regarding the implementation of the core condition as sketched in Sec. II, the main conclusion of Ref. 19 was that

a minimum of  $N_{cc}=7$  basis functions in addition to  $u_0$  were necessary for acceptable results despite residual defects of  $g(r)$  close to the origin; a short discussion of the core condition's slightly different role for square wells will be presented below (Sec. IV B).

The critical density  $\varrho_c$  predicted by HRT, it should be noted, is virtually always in reasonable agreement with literature data as shortly presented in Sec. IV A; indeed, HRT is even able to reproduce the marked rise in  $\varrho_c$  predicted by Refs. 21, 27, and 29 for  $\lambda \rightarrow 1+$  as opposed to the rigorously constant value in Ref. 28. Due to the satisfactory  $\varrho_c$  values obtained numerically we will henceforth exclude  $\varrho_c$  from the discussion; for a demonstration of both  $\varrho_c$ 's insensitivity to variation of parameters of the numerical procedure and the quantitative agreement with the data of Sec. IV A see Figs. 1 and 2.

In this context it may be of interest that the HRT estimate for the critical density presents no difficulties for the hard-core Yukawa fluid considered in Ref. 19, either, nor is there any mention of such difficulties in any of the other publications on this topic that we are aware of; indeed, the theory's numerical problems primarily lie in the solution's small- $Q$  behavior for close-to-critical and subcritical temperatures on the one hand and the use of mutually incompatible assumptions prompted by the need to employ decoupling without giving up thermodynamic consistency on the other hand. Both of these aspects of HRT pertain to different parts of the  $(Q, \varrho)$  plane, located close to the high-density boundary for the role mathematical inconsistencies play and at not too large  $Q$  and  $\varrho \sim \varrho_c$  for the pathological behavior related to coexistence; they will be discussed in Secs. IV C and IV D, respectively, and their vestiges will also be seen in the results of applying HRT in the formulation of Sec. II to square wells of quasicontinually varying range  $\lambda \in ]1, 3.6]$  in Sec. IV E.

##### A. Non-HRT results for square wells

For comparison purposes we have collected in Tables I and II the critical temperatures of various square well systems as obtained from simulations (Table I) or by purely theoretical means (Table II); the data included have been published within the last decade.

Of the simulation based results included in Table I, only those of Ref. 26 for  $\lambda \in \{1.25, 1.375, 1.5, 1.75, 2\}$  have been obtained by molecular dynamics (MD); most of the other simulation studies rely on one or the other variant of the Monte Carlo (MC) method: Among these, the Gibbs ensemble MC (GEMC) calculations of Ref. 21 set out to determine critical exponents,  $\beta$  in particular; that work's finding of  $\beta \sim 1/2$  for  $\lambda = 2$  as opposed to the expected  $\beta \sim 1/3$  found for  $\lambda$  up to 1.75 prompted reexamination of the square well fluid with  $\lambda = 2$  by GEMC augmented by finite-size scaling (FSS) techniques,<sup>22</sup> refuting the mean field value for the effective exponent.

Especially in the critical regime, grand canonical MC (GCMC) simulations incorporating histogram reweighting and FSS offer some advantage over GEMC due to the latter's restriction to fixed temperature; such an approach has been applied to square wells with  $\lambda = 1.5$  and 3 in Ref. 23; a more

elaborate GCMC scheme not biased towards the Ising universality class and taking into account the YY anomaly has recently been applied to<sup>31</sup>  $\lambda = 1.5$ , see above. Yet another method goes under the name of thermodynamic- or temperature-and-density-scaling MC (TDSMC); it was applied to the case of  $\lambda = 1.5$  and analyzed in terms of an effective Hamiltonian in Refs. 24 and 25.

Also included in Table I are the results of Ref. 27, employing a MC scheme modified to take advantage of a speed-up possible by combining simulation data with an analytical *ansatz* for the chemical potential; the efficiency of this approach originally devised to study phase separation allows a large number of systems to be considered. (The error bounds given for these “modified MC” results in Table I have been obtained from the different results displayed in Ref. 27 for different parameter settings.)

The theoretical predictions for the critical temperature listed in Table II comprise a second-order analytic perturbation theory<sup>29</sup> (APT2) applicable to  $1 < \lambda \leq 2$  and claimed accurate for  $\lambda \geq 1.4$  as well as the hard-sphere van der Waals (HSvdW) equation of state.<sup>28</sup> In addition, though not listed in Table II, we have utilized the non-square-well-specific Okumura-Yonezawa (OY) estimate<sup>50</sup> for  $\beta_c$ , primarily as a starting value when looking for the critical temperature in our HRT calculations; for  $v^{\text{sw}[-\epsilon, \lambda, \sigma]}$ , the OY prediction is  $k_B T_c / \epsilon = 0.425 \lambda^3 - 0.273$ .

## B. The core condition

Ever since application of HRT to continuous fluids started, the implementation of the core condition has been a major issue, probably motivating adoption of the closure (4) and variants thereof for non-hard-sphere reference systems<sup>16</sup> despite its known deficiencies in the first place; indeed, it is no coincidence that several studies<sup>7,11,15,18</sup> primarily concerned with the RG aspect of the theory chose to completely eliminate the core condition. When applying HRT as a regular liquid state theory, on the other hand, this is not an option: too great is the effect this may have on both correlation functions and phase behavior.<sup>19</sup> From Table III where we compile the critical temperature  $T_c = 1/k_B \beta_c$  for various square well potentials as functions of the number  $N_{\text{cc}} + 1$  of basis functions in the closure (4), just as in Ref. 19 we find virtually constant critical temperatures for  $1 \leq N_{\text{cc}} \leq 4$ ; on the other hand, the amount of variation seen upon further increasing  $N_{\text{cc}}$  strongly depends on  $\lambda$ , which immediately carries over to the pair distribution function  $g^{(Q_0)}(r, \varrho)$  and its compatibility with the core condition: For  $\lambda = 3$ , the longest-ranged potential considered in Table III,  $g^{(Q_0)}(r, \varrho) = 0$ ,  $r < \sigma$ , holds reasonably well except very close to  $r = 0$  even for  $N_{\text{cc}} = 1$ ; when increasing the number of basis functions all the way to  $N_{\text{cc}} = 10$ , the pair distribution function has to be corrected for very small  $r$  only, yielding a  $|g^{(Q_0)}(r, \varrho)|$  that remains bounded by some  $10^{-2}$  of the contact value  $g^{(Q_0)}(\sigma+, \varrho)$  for all  $r < \sigma$ ; the corresponding small change in  $g^{(Q_0)}(r, \varrho)$  and  $C^{(Q_0)}(r, \varrho)$  is reflected in the near-constant predictions for  $\beta_c$  evident from Table III.

Similarly, for  $\lambda = 1.5$  and  $\lambda = 2$  and within the  $N_{\text{cc}}$  range considered, the implementation of the core condition does not convincingly improve except for supercritical tempera-

TABLE I. The critical temperature  $T_c$  of square well systems for various values of  $\lambda$  as predicted by simulations and simulation-based theoretical analyses, and the corresponding references. The acronyms used for labeling the method employed in obtaining these results are given in Sec. IV A of the text.

$\lambda$	$k_B T_c(\lambda) / \epsilon$	Method
1.05	0.3751(1)	mod. MC (Ref. 27)
1.1	0.4912(4)	mod. MC (Ref. 27)
1.15	0.5942(35)	mod. MC (Ref. 27)
1.2	0.692(1)	mod. MC (Ref. 27)
1.250	0.764(4)	GEMC (Ref. 21)
1.25	0.78	MD (Ref. 26)
	0.7880(6)	mod. MC (Ref. 27)
1.3	0.8857(7)	mod. MC (Ref. 27)
1.375	0.974(10)	GEMC (Ref. 21)
	1.01	MD (Ref. 26)
1.4	1.076(8)	mod. MC (Ref. 27)
1.5	1.2179(3)	GCMC(YY) (Ref. 31)
	1.2180(2)	GCMC (Ref. 23)
	1.219(8)	GEMC (Ref. 21)
	1.222	TDSMC (Refs. 24 and 25)
	1.226	TDSMC (Refs. 24 and 25)
	1.246(5)	TDSMC (Refs. 24 and 25)
	1.27	MD (Ref. 26)
	1.302(8)	mod. MC (Ref. 27)
1.65	1.645(5)	mod. MC (Ref. 27)
1.75	1.79	MD (Ref. 26)
	1.811(13)	GEMC (Ref. 21)
1.8	2.062(8)	mod. MC (Ref. 27)
2	2.61	MD (Ref. 26)
	2.648(14)	GEMC+FSS (Ref. 22)
	2.666(85)	GEMC+FSS (Ref. 22)
	2.678(27)	GEMC+FSS (Ref. 22)
	2.6821(8)	GEMC+FSS (Ref. 22)
	2.684(51)	GEMC+FSS (Ref. 22)
	2.721(89)	GEMC+FSS (Ref. 22)
	2.730(14)	GEMC+FSS (Ref. 22)
	2.764(23)	GEMC (Ref. 21)
	2.778(7)	mod. MC (Ref. 27)
2.2	3.80(1)	mod. MC (Ref. 27)
2.4	5.08(2)	mod. MC (Ref. 27)
3	9.87(1)	GCMC (Ref. 23)

tures and intermediate densities; this time, however, the pair distribution functions remain far from compatible with the core condition even for  $N_{\text{cc}} = 10$ , and neither  $\beta_c$  nor  $g^{(Q_0)}(r, \varrho)$  itself nor, for that matter, the final values of the LOGA/ORPA expansion coefficients  $\gamma_n^{(Q_0)}(\varrho)$  indicate that the expansion (4) for  $\tilde{C}^{(Q)}(k, \varrho)$  might be close to convergence. But if the quality of  $g^{(Q_0)}(r, \varrho)$  improves only little if at all, the remaining deficiencies are probably to be blamed on the approximation for the poorly convergent integrals' derivative with respect to  $Q$  mentioned earlier [cf. Eq. (12) of Ref. 19] rather than on an insufficient number of basis functions; on the other hand, even though the decoupling assumption cannot directly affect the pair distribution function's compliance with the core condition, the approximation of neglecting the non-local term in  $\partial \hat{T}^{(Q)}[\psi(k, \varrho), \varrho] / \partial Q$  is on the same level as that of setting  $\alpha^{(Q)}(\varrho) = 0$ , as was stressed by the authors of Ref. 8 upon jointly introducing these two assumptions. Thus, combining the above findings regarding the core condition with the analogous analysis of Sec. IV of Ref. 19 and with that contribution's investigation

TABLE II. The critical temperature  $T_c$  of square well systems for various values of  $\lambda$  as predicted by purely theoretical means, and the corresponding references. The acronyms used for labeling the method employed in obtaining these results are given in Sec. IV A of the text.

$\lambda$	$k_B T_c(\lambda)/\epsilon$	Method
1.125	0.587	APT2 (Ref. 29)
1.25	0.751	HSvdW (Ref. 28)
	0.850	APT2 (Ref. 29)
1.375	0.978	HSvdW (Ref. 28)
	1.08	APT2 (Ref. 29)
1.5	1.249	HSvdW (Ref. 28)
	1.33	APT2 (Ref. 29)
1.625	1.61	APT2 (Ref. 29)
1.75	1.859	HSvdW (Ref. 28)
	1.93	APT2 (Ref. 29)
1.85	2.23	APT2 (Ref. 29)
2	2.506	HSvdW (Ref. 28)
	2.79	APT2 (Ref. 29)

into the decoupling assumption’s possible effect (cf. Fig. 2 of Ref. 19) we are led to the conclusion that decoupling poses certainly no less a problem here than for the hard-core Yukawa potential studied there.

### C. High-density boundary condition

Numerically, there are two ways for the implementation of Sec. III to fail to reach  $Q = Q_0$ , both, of course, easily detected by the “monitoring” variant of our code (cf. Sec. III E of Ref. 19): due to the solution’s pathological behavior wherever  $f(Q, \varrho)$  is large (cf. Sec. IV D), or because of inappropriate boundary conditions at high density. As for the latter—an issue intimately linked to the decoupling assumption—the immediate reason for the program’s failure is a near-discontinuity in the numerical solution close to the boundary: For the moment setting aside the decoupling assumption and other approximations, in the application of HRT with the closure (4) at any point  $(Q, \varrho)$  in the interior of the PDE’s domain the core condition uniquely determines the  $\gamma_n^{(Q)}(\varrho)$ ,  $n \geq 1$ , for given  $\gamma_0^{(Q)}(\varrho)$ ; this expansion coefficient is then determined by imposing thermodynamic consistency as embodied in the compressibility sum rule (3). At a boundary, i.e., for  $\varrho \in \{\varrho_{\min}, \varrho_{\max}\}$ , however, the second density derivative cannot be evaluated reliably so that some other condition must be imposed; in the calculations reported here (with the obvious exception of those for Fig. 4) we always choose  $\varrho_{\min} = 0$  so that the divergence of the ideal gas term in  $\tilde{C}^{(Q)}$  provides  $f(Q, \varrho) = 0$  as a convenient and unproblematic boundary condition. For  $\varrho = \varrho_{\max}$ , on the other hand, we are in principle free to use any suitable approximation for the structural and thermodynamic properties of the  $Q$  system and to calculate  $f(Q, \varrho_{\max})$  from said approximation, thereby providing the necessary boundary condition for the PDE (6); but for practical reasons it is desirable to use the same LOGA/ORPA form for the  $Q$  system’s direct correlation function at  $\varrho_{\max}$  as in the rest of the problem’s domain so that, in particular, the LOGA/ORPA prescription  $\gamma_0^{(Q)}(\varrho_{\max}) = 0$  is a natural choice of boundary condition. In general, however, due to the PDE’s diffusion like character any condition imposed at  $\varrho_{\max}$  that is incompatible with the

TABLE III. The dependence of the critical temperature of square well systems on the number  $N_{cc} + 1$  of basis functions retained in Eqs. (4) and (5) for various values of  $\lambda$ . For  $N_{cc} > 0$ , the decoupling assumption was imposed as high-density boundary condition, whereas the LOGA/ORPA condition  $\gamma_0^{(Q)}(\varrho_{\max}) = 0$  served the same purpose for  $N_{cc} = 0$ ; other parameters were chosen as indicated in Sec. III.

$N_{cc}$	$k_B T_c(\lambda = 1.5)/\epsilon$	$k_B T_c(\lambda = 2)/\epsilon$	$k_B T_c(\lambda = 3)/\epsilon$
0	1.209 437(035)	2.660 946(132)	9.891 032(298)
1	1.190 663(034)	2.682 489(105)	9.899 937(478)
2	1.203 326(035)	2.686 289(105)	9.900 894(478)
3	1.200 152(035)	2.686 078(105)	9.900 894(478)
4	1.197 136(034)	2.685 655(105)	9.900 894(478)
5	1.287 443(040)	2.527 365(093)	9.737 080(462)
6	1.098 329(029)	2.742 404(110)	9.822 071(471)
7	0.984 757(047)	2.914 763(124)	9.867 502(475)
8	1.070 878(027)	2.744 830(110)	9.773 324(466)
9	1.216 333(036)	2.749 695(110)	9.887 510(477)
10	1.207 583(035)	2.937 591(126)	9.748 203(464)

solution for  $\varrho < \varrho_{\max}$  by necessity induces a corresponding near-discontinuity in  $f(Q, \varrho)$  close to the boundary; within the framework of a finite-difference scheme this is reflected in a mismatch of  $f(Q, \varrho_{\max})$  and the solution at densities close by, i.e.,  $f(Q, \varrho_{\max} - i\Delta\varrho)$  for small  $i \geq 1$ , and the mismatch’s severity may serve as a direct measure for the inappropriateness of the boundary condition at  $\varrho_{\max}$  in relation to the approximations applied at densities in  $]\varrho_{\min}, \varrho_{\max}[$ .

On the other hand, the numerics become intractable unless we adopt the decoupling assumption, and the only way to consistently use  $\alpha^{(Q)}(\varrho) = 0$  without abandoning the core condition is to decouple the HRT-PDE to a set of ODEs at fixed density only;<sup>19</sup> this, unfortunately, removes all traces of thermodynamic consistency from the equations and thereby precludes obtaining clear phase boundaries.<sup>19</sup> It is therefore necessary to restrict decoupling to the implementation of the core condition only while retaining the structure of a PDE together with the compressibility sum rule (3) despite the latter’s incompatibility with decoupling. Thus, for  $\varrho_{\min} < \varrho < \varrho_{\max}$ , both  $\tilde{C}^{(Q)}(0, \varrho) = -\partial^2(\beta A^{(Q)}/V)/\partial\varrho^2$  and  $\alpha^{(Q)}(\varrho) = 0$  are used for different parts of the problem; at  $\varrho_{\max}$ , however, again any approximation allowing calculation of  $f(Q, \varrho_{\max})$  may be used, so that it is tempting to once again resort to the LOGA/ORPA condition of vanishing  $\gamma_0^{(Q)}(\varrho_{\max})$  or variants thereof.

But due to the decoupling assumption’s possibly large effect, any boundary condition that does not incorporate  $\alpha^{(Q)}(\varrho_{\max}) = 0$ —and bear in mind that  $\gamma_0^{(Q)}(\varrho_{\max})$  and  $\alpha^{(Q)}(\varrho_{\max})$  cannot both vanish at the same time for generic cutoff  $Q$ —will once again incur a fatally large mismatch; if, however, we must resort to decoupling anyway, it seems preferable to consistently apply it for the boundary condition rather than to inconsistently combine it with a condition alien to the theory; also, though the mismatches’ magnitudes from imposing  $\alpha^{(Q)}(\varrho_{\max}) = 0$  alone or from mixing it with the LOGA/ORPA condition  $\gamma_0^{(Q)}(\varrho_{\max}) = 0$  generally do not differ much as long as the PDE’s stiffness does not play a role (e.g., for  $\lambda = 1.5$ , as long as we restrict ourselves to  $Q \sim 8/\sigma$  or higher, or to  $\beta \leq \beta_c$ ), the former approach fares better than the other one more often than not. It is only in

this sense, i.e., presupposing a LOGA/ORPA-like *ansatz* even at  $\varrho_{\max}$  and application of decoupling in the implementation of the core condition according to Eq. (5) at all  $\varrho$ , that the results are largely independent of the choice of boundary condition as claimed, for  $\beta < \beta_c$ , in Ref. 8.

In the numerical work we find that such a mismatch is present whenever the calculation proceeds via mathematically inconsistent or conflicting approximations; in the case of square wells with their comparatively short potential range, however, the problems are much more severe than in other systems so that  $\beta_{\max, \#}$  is rather small and even drops below  $\beta_c$  for most of the  $\lambda$  interval from 1 to 2 (cf. Sec. IV E). Restricting ourselves to  $\beta < \beta_{\max, \#}$  and  $Q = Q_0$ , the mismatch is typically reflected in an increase by one order of magnitude in the three-point finite-difference estimate of, e.g.,  $|\partial^2 f(Q_0, \varrho) / \partial \varrho^2|$  right at the boundary over the near-constant values at slightly lower densities; apart from a positive correlation with  $\epsilon_{\#}$ , the mismatch's severity is qualitatively unaffected by a change in parameters of the numerical procedure or the choice and location of the boundary condition (with the above provisions).

Another effect worth mentioning in connection with the boundaries is the influence their locations, viz.,  $\varrho_{\min}$  and  $\varrho_{\max}$ , may have. The basic mechanism and its implications for the coexisting densities were already mentioned in the opening remarks of this section; here we only want to point out that the noncriticality enforced by the boundary conditions not only may unduly distort the binodal predicted by HRT as demonstrated in Fig. 1, very small  $\varrho_{\max}$  may also allow one to reach  $Q = Q_0$  at higher  $\beta$ , thus effectively raising  $\beta_{\max, \#}$  while lowering  $\beta_{\max}$ .

Sometimes, however, the expectation of the binodal keeping a separation from the boundary of several  $\Delta \varrho$  at least does not hold, and a preposterous two-phase region appears very close to  $\varrho_{\max}$  or, very rarely, close to  $\varrho_{\min}$ ; e.g., for  $\lambda = 1.88$  and  $\beta = 0.392/\epsilon$  the equations can be solved all the way down to  $Q = Q_0 = 10^{-4}/\sigma$ , predicting an unrealistic two-phase region extending from  $0.845(5)/\sigma^3$  to  $0.995(5)/\sigma^3$ . This behavior turns out to come from the in-

terplay of the mismatch at  $\varrho_{\max}$  and the numerical treatment of the stiffness of the PDE.

#### D. The region of large $f(Q, \varrho)$

For subcritical temperatures the HRT-PDE's true solution's erratic behavior in that part of the  $(Q, \varrho)$  plane where  $f(Q, \varrho)$  is large and the isothermal compressibility's divergence is built up (cf. Sec. II, q.v. Ref. 20) obviously eludes reliable numerical realization; in particular, while  $\epsilon_{\#}$  still characterizes the level of accuracy in auxiliary calculations, the same can no longer be true for the accuracy of the PDE's discretization as this would require step sizes  $\Delta Q$  so small as to cause floating point underflow upon evaluating, e.g.,  $Q - (Q - \Delta Q)$ , thus rendering finite differences numerically insignificant.

Consequently, in this respect we have to give up our strategy of controlling the numerical procedure so as to locally ensure a quality of  $\epsilon_{\#}$  at least, turning to predetermined step sizes<sup>19</sup>  $\Delta Q$  in addition to fixed  $\Delta \varrho$ , to which similar concerns apply;<sup>20</sup> on such a coarse mesh of  $(Q, \varrho)$  points underlying the finite-difference scheme, however, the true solution cannot even be represented adequately, and the numerical approximation for  $f(Q, \varrho)$  obtained from the PDE's discretization with these far too large step sizes cannot be trusted to faithfully represent even the average behavior of  $f(Q, \varrho)$ .

This inadequacy of the step sizes is reflected in various peculiarities of the solution vector obtained in the numerical procedure; indeed, when monitoring the evolution of  $f(Q, \varrho)$  and the core condition coefficients  $\gamma_n^{(Q)}(\varrho)$ , our code readily detects the plummeting step sizes necessary and signals the incompatibility of the behavior seen with the assumption of smoothness underlying finite-difference schemes. Another telltale sign is iterated corrector steps' failure to converge when  $f(Q, \varrho)$  is large: even though implicit schemes like the one we employ<sup>20</sup> are the standard treatment for stiff systems, the rapid growth of the oscillations' amplitudes renders the finite-difference equations themselves unstable under itera-

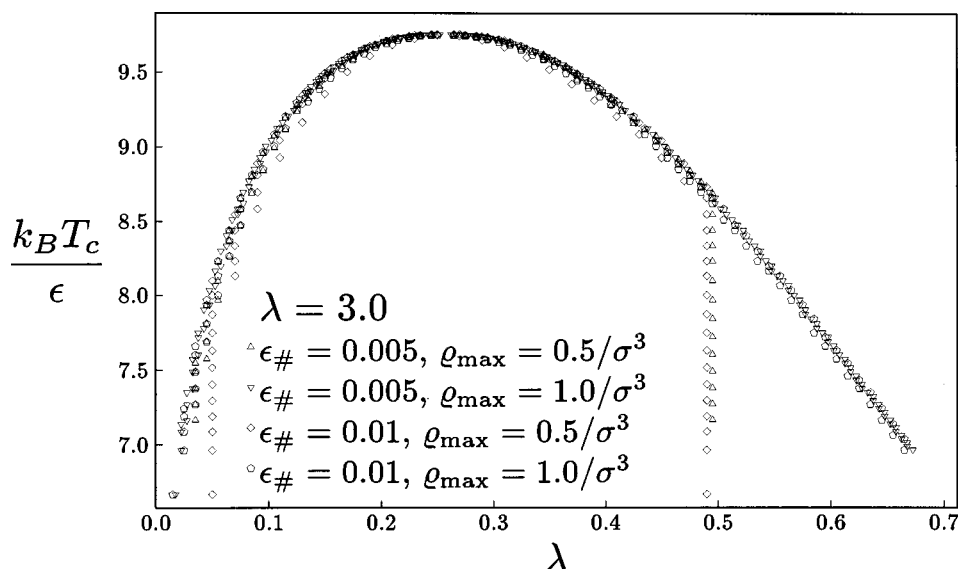


FIG. 1. The binodal of the square well system with  $\lambda = 3$  as obtained for different values of  $\epsilon_{\#}$  and  $\varrho_{\max}$ ; cf. the discussion in Sec. IV C. Note that for this rather long-ranged system the critical point's location is virtually unaffected by variation of these parameters. Also, imposing the boundary condition at  $\varrho_{\max} = 0.5/\sigma^3$  clearly induces a shift in  $\varrho_v$  to higher and, to a lesser degree, in  $\varrho_l$  to lower values even well above the temperature where  $\varrho_l$  gets close to  $\varrho_{\max}$ , which is readily interpreted as an effect brought about by stiffness; the results for  $\varrho_{\max} = 0.5/\sigma^3$  and  $\epsilon_{\#} = 0.005$  do not differ much from those with the same  $\varrho_{\max}$  and  $\epsilon_{\#} = 0.01$  except in the binodal's vapor branch's shift being somewhat smaller.



tion; only when resigning on any control of the numerical error and refraining from iterations of the corrector step do the step sizes  $\Delta Q$  chosen allow one to force advancing  $Q$  all the way to  $Q_0$  in remarkably many cases. Also, comparison of  $f(Q_0, \varrho)$  as obtained with different sets of step sizes  $\Delta Q$  reveals that, for  $\varrho_v < \varrho < \varrho_l$ , the evolution of  $f(Q, \varrho)$  seen numerically is driven by the number and size of  $Q$  steps only and certainly does not correspond to an average over oscillations;<sup>20</sup> the same mechanism is also responsible for a small  $\Delta Q$  dependence of the critical temperature  $\beta_c$ .

By the same token, due to the  $d_{01}$  and  $d_{02}$  terms in Eq. (6), the PDE's stiffness and the related problems have a direct bearing on the solution outside the coexistence region even if the numerical predictions there turn out rather insensitive to variation of parameters of the numerical procedure; in particular, we expect a gradual but non-negligible distortion (in addition to the effects of numerical differentiation close to the near-discontinuity) of the binodal, increasing with falling temperature.

### E. HRT results for square wells

In light of the preceding exposition as well as of the discussion in Ref. 19 it may at first seem surprising that HRT in the formulation of Sec. II has a record of being highly applicable to a variety of systems (cf. Sec. I); also, as we shall see in a moment, even for square wells, a system expected to be particularly vulnerable to the problems just outlined, we find reasonable estimates of the critical points' locations for a wide range of  $\lambda$  values. Still, the mechanisms sketched in Secs. IV C and IV D as well as the difficulties presented in Ref. 19 remain and manifest themselves numerically in a number of ways.

For a first orientation, let us look at the results summarized in Figs. 2 and 3 where the critical temperature  $T_c$  and density  $\varrho_c$  are shown as functions of  $\lambda$ ; the underlying calculations have been obtained with  $\epsilon_{\#} = 10^{-2}$ , imposing decoupling in a consistent way at  $\varrho_{\max} = 1/\sigma^3$  and with  $N_{cc} + 1 = 7 + 1$  basis functions in the expansion (4) of the LOGA/ORPA function  $\mathcal{G}^{(Q)}$ . With the exception of some spurious results at  $\lambda \sim 1.1$ , wherever  $\beta_c < \beta_{\max, \#}$  the critical temperature in general compares quite favorably with the data of Tables I and II; from the calculations we have performed for a large number of systems in the range  $1 < \lambda \leq 3.6$  and ignoring some isolated results, a critical point is found for  $1.06 \leq \lambda \leq 1.24$ , for  $1.45 \leq \lambda \leq 1.53$ , and for  $\lambda \geq 1.939$ ; calculations with  $N_{cc} = 5$  yield analogous results,<sup>20</sup> with  $\beta_c < \beta_{\max, \#}$  in a somewhat larger part of the parameter range, viz., for  $1.09 \leq \lambda \leq 1.58$  and for  $\lambda \geq 1.896$ , but will not be considered in the following in view of the considerations of Sec. IV B and of other defects that turn out to be larger than for  $N_{cc} = 7$ .

For the moment setting aside the data for  $\lambda < 1.939$ , HRT's predictions for the critical temperature are generally found to be in satisfactory agreement with the  $\beta_c(\lambda)$  curve expected from the simulation-based and theoretical results presented in Sec. IV A. Embedded into this regular overall behavior of  $\beta_c$  as a function of  $\lambda$ , however, we find a number of depressions and elevations of  $\beta_c$ , some of which cannot be seen on the scale of Fig. 2 but from the numeric results

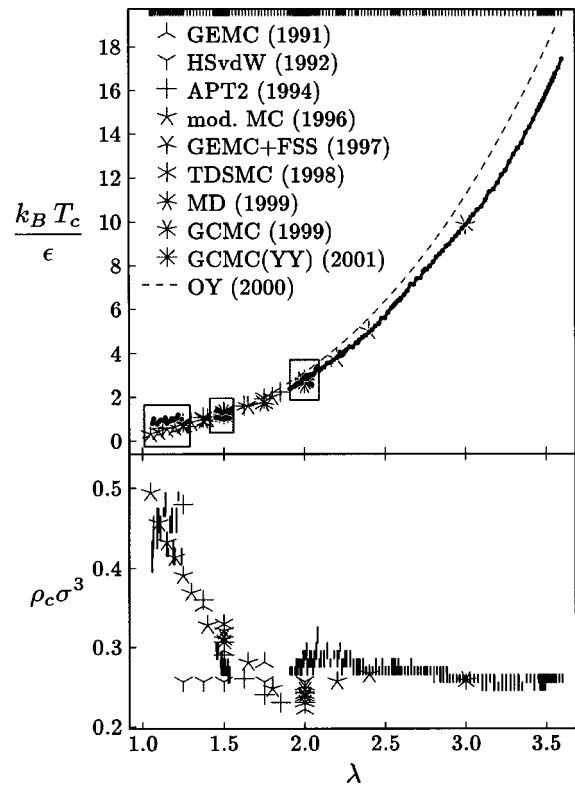


FIG. 2. The critical temperature  $T_c$  (dots in upper panel) and critical density  $\varrho_c$  (bars in lower panel) of square well systems for  $\lambda$  ranging from close to unity up to 3.6 as obtained from calculations with parameters chosen as indicated in Sec. III; also included are the non-HRT predictions listed in Tables I and II, labeled by the acronyms introduced in Sec. IV A and already used in those tables. The ticks on the top border of the figure's frame indicate the  $\lambda$  values considered; of the 200-odd systems we looked at,  $\beta_{\max, \#}$  exceeded  $\beta_c$  only in the  $\lambda$  ranges indicated in Sec. IV E or for some isolated  $\lambda$  values outside those ranges. The three boxes in the upper panel indicate the parameter ranges displayed at larger scale in Fig. 3. In the lower panel, the bars show the coexisting densities found according to the prescriptions of Sec. III for the highest-temperature subcritical isotherm calculated in locating the critical temperature, which explains the apparent differences in  $\varrho_c$ 's accuracy; the smallest  $\varrho_c$  intervals shown coincide with the spacing  $\Delta \varrho = 10^{-2}/\sigma^3$  of the density grid.

only;<sup>20</sup> others, however, are so strong as to render the critical temperature a nonmonotonic function of  $\lambda$ , which is certainly not expected on the grounds of the literature presented in Sec. IV A, the data of Refs. 27–29 in particular.

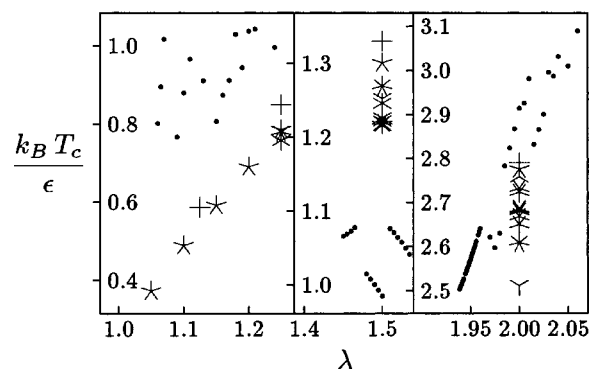


FIG. 3. The critical temperature data of Fig. 2 for values of the square well range parameter  $\lambda$  close to 1.1, 1.5, and 2 at larger scale; the symbols coincide with those used in Fig. 2.

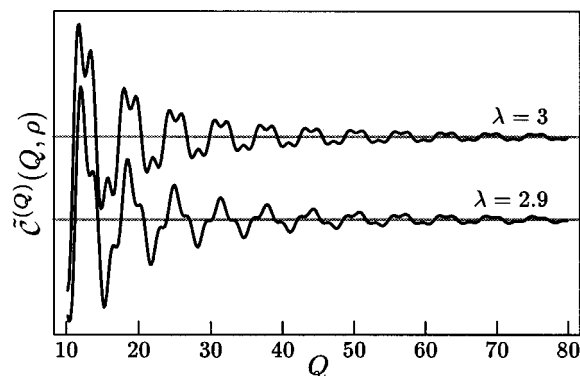


FIG. 4. The core-condition function  $\tilde{c}^{(Q)}(Q, \varrho)$  for  $\varrho = 0.3/\sigma^3$ ,  $\beta = 0.2/\epsilon$  and for two different ranges  $\lambda$  of the square well potential, on arbitrary scales; the horizontal lines correspond to the ideal gas value  $-1/\varrho$ . Note that, for  $\lambda = 3$  (upper curve), the peak of every single one of the function's swings is partially reduced, which is the case less than half the time—and at rather high  $Q$  only—for  $\lambda = 2.9$  (lower curve). We have excluded the data for  $Q < 10/\sigma$  so that the effects of the PDE's stiffness are still negligible; the underlying calculations have been performed by solving the ODEs corresponding to consistent application of the decoupling assumption at the density indicated.

In light of Sec. IV D it is of course tempting to simply attribute this behavior to the difficulties previously discussed, especially since the critical point is located in the region of large  $f(Q_0, \varrho)$  by definition; the peculiar distribution of  $\lambda$  values affected, however, suggests that these problems of the numerical procedure are triggered by a special mechanism. Indeed, a closer look at the core condition function  $\tilde{c}^{(Q)}(Q, \varrho)$  for fixed density  $\varrho$  reveals, for every single one of the  $\lambda$  values implicated that we checked, that the combination of terms pertaining to  $w(r)$  or  $v^{\text{hs}}(r)$  alone (of ranges  $\lambda\sigma$  and  $\sigma$ , respectively) regularly and quite frequently reduces the amplitude of this function's swings about the ideal gas value of  $-1/\varrho$ ; the same happens only occasionally for  $\lambda$  values removed from these irregularities so that it is, in fact, possible to quite reliably determine whether or not a given  $\lambda$  is affected from a plot of  $\tilde{c}^{(Q)}(Q, \varrho)$  for  $\varrho \sim \varrho_c$  alone as illustrated in Fig. 4. It will come as no surprise that most of the irregularities occur when  $\lambda$ , the ratio of the two characteristic lengths present in the model, is close to a simple fraction: among the shifts in  $T_c$  most obvious are those where  $\lambda$  is close to 2 (cf. Fig. 3),  $2\frac{1}{4}$ ,  $2\frac{1}{7}$ ,  $2\frac{1}{9}$ , and  $2\frac{1}{12}$ , and in retrospect it seems justified to also include the small parameter range around  $\lambda = 1\frac{1}{2}$  in this list, see below; the effect is less obvious from Fig. 2 but still discernible at  $2\frac{1}{2}$ ,  $2\frac{1}{3}$ , and  $2\frac{2}{3}$ , whereas for  $2\frac{1}{4}$  and  $2\frac{3}{4}$  it is so small as to make the plot of  $\beta_c(\lambda)$  appear smooth while the irregularities are still evident from the numerical values; also note that, once again,  $\varrho_c$  is hardly affected.

All these observations seem to indicate that indeed it is the interplay of the two different length scales and the resulting partial oppression of a significant portion of the oscillations of  $\tilde{c}^{(Q)}(Q, \varrho)$  that cause the discrepancy of HRT and literature results for the critical temperature around certain  $\lambda$  values even though a smooth interpolation of HRT's predictions from  $\lambda$  values nearby is well compatible with the data

presented in Sec. IV A. Even though we currently cannot pinpoint the precise mechanism by which this unphysical behavior of HRT arises and, in particular, cannot distinguish between the closure's inadequacy and the PDE's stiffness as the main culprit—though the latter is certainly implicated to some degree—two conclusions may be drawn quite safely: for one, as long as we stay clear of values of  $\lambda \geq 2$  that are close to simple fractions, or restrict ourselves to  $\lambda \geq 2.7$  where the effects are rather small, we can probably trust the numerical results—with the *caveats* of Ref. 19 and Secs. IV C and IV D—to the same degree of confidence as those obtained for the hard-core Yukawa system in Ref. 19. And secondly, it is only in the presence of discontinuities in the potential that certain lengths feature prominently in the relevant functions' Fourier transforms and can so give rise to problems of the kind outlined above; consequently, as long as we confine ourselves to continuous  $w(r, \varrho)$ , which still includes most of the potentials popular in liquid state physics, the unphysical shifts in  $\beta_c$  seen for certain parameter combinations are likely not an issue, whereas the same problems are expected to resurface, e.g., for the multistep potential also defined in Sec. III B of Ref. 19.

Another lesson to be drawn from the findings presented here as well as in Ref. 19 is that, as a general rule, conclusions should never be drawn from isolated results alone; it is only through the combination and meticulous scrutiny of a set of related calculations that meaningful information can be extracted from HRT calculations: due to the problems related to the implementation of the core condition, to the nature and location of the boundary conditions, and to the PDE's stiffness, any single calculation must be considered as of uncertain standing. As an example,<sup>20</sup> the analog of Fig. 1 for  $\lambda = 1.5$  shows a considerably larger variation in the binodal and the critical point's location, which is consistent with the above conclusions regarding the reason for  $\beta_{\text{max},\#}$  rising above  $\beta_c$  in a narrow region around this  $\lambda$  value, whereas any one of the phase boundaries found in itself is a perfectly plausible candidate for the “true” HRT binodal.

## V. CONCLUSION

In conjunction with the findings of Ref. 19, the discussion of Sec. IV provides quite coherent a picture of HRT's numerical side as well as of some peculiarities encountered for square wells. Most prominently, we see a marked dependence of the quality of the results on the potential's range, confirming the trend of decreasing accuracy for narrower potentials reported<sup>47</sup> for the hard-core Yukawa fluid; it has long been accepted<sup>6,13,47</sup> that the simplistic but computationally convenient<sup>19</sup> closure (4) has a part in this, and an improved closure has recently been proposed.<sup>51</sup> Still, as far as numerical application of HRT is concerned, the closure cannot be discussed without reference to the decoupling assumption and to the approximate implementation of the core condition via ODEs coupled to the HRT-PDE; while the former has been found problematic both for square wells (present contribution) and for the hard-core Yukawa fluid considered in Ref. 19 and should probably not be trusted easily for any system, the severity of the difficulties brought about by the simplified treatment of the core condition sensitively de-

depends on the potential type and parameters chosen: for the continuous and rather long-ranged Yukawa potential with  $z = 1.8/\sigma$ ,  $g^{(Q_0)}(r, Q)$  can be made sufficiently small within the core, and the square well fluid with  $\lambda = 3$  fares equally well at least. From the discussion of Sec. IV B and the data of Table III, however, it becomes apparent that smaller  $\lambda$ —we have looked at  $\lambda = 1.5$  and  $\lambda = 2$  in particular—incurs substantial problems, with residual defects in the pair distribution functions attributed to the ill-justified approximation of neglecting some slowly converging integrals<sup>19,20</sup> in the core condition, but Table III demonstrates not only the  $\lambda$  dependence of the results' sensitivity to the number  $N_{cc} + 1$  of basis functions retained in the truncated equation (5) when varying  $N_{cc}$  in the range  $0 \leq N_{cc} \leq 10$ : while the virtually constant critical temperature predicted for  $\lambda = 3$  seems trustworthy and is, indeed, well compatible with simulation results (cf. Table I), the amount of variation in  $\beta_c$  for  $\lambda = 1.5$  and, to a much lesser degree, for  $\lambda = 2$  precludes accurate determination of the critical temperature; this is a first indication that the theory might be able to handle square wells with  $\lambda = 3$  quite reliably, whereas problems cannot be denied for  $\lambda = 2$ , and  $\lambda = 1.5$  seems largely out of reach for HRT in the present formulation. This is confirmed by the results obtained by quasicontinuous variation of  $\lambda$  in the range  $1 < \lambda \leq 3.6$  as shown, for  $N_{cc} = 7$ , in Fig. 2: the critical point is accessible only in part of this parameter range, and not only the critical temperature at fixed  $\lambda$  but also the boundaries of the  $\lambda$  intervals where HRT is able to reach temperatures as low as  $T_c$  strongly depend on  $N_{cc}$  (cf. Sec. IV E).

Applicability of HRT to only a restricted  $\lambda$  range is, of course, again related to the pronounced short-rangedness of the square well potential; to explain it, however, we have to invoke not only the LOGA/ORPA-style closure and the approximate implementation of the core condition but also the other difficulties encountered in the numerical procedure as highlighted in this and our previous contribution, viz., the decoupling assumption (Ref. 19), inappropriate boundary conditions (Sec. IV C) and, most importantly, the PDE's stiffness for thermodynamic states of high compressibility (Sec. IV D). All of these are, in principle, always present to some degree in numerical applications of HRT; it may prove valuable that Secs. IV C and IV D provide distinct signatures readily detected by the implementation of Sec. III that might be looked out for in more advanced applications of the theory, too.

Related to these difficulties is a peculiar effect specific to square wells (Sec. IV E): close to certain  $\lambda$  values, simple fractions in particular, we see shifts in the critical temperature that render HRT's predictions much less compatible with simulations and other theoretical descriptions of the square well fluid than would be expected from the results obtained for  $\lambda$  values close by; the mechanism for triggering these local distortions of the  $\beta_c(\lambda)$  curve is illuminated at least to the point of linking it to the presence of a discontinuity in the potential's perturbational part. All in all, the numerical evidence as well as comparison with literature data suggest that the formulation of HRT sketched in Sec. II is well able to deal with square wells and to locate their critical points to

reasonable accuracy for  $\lambda \geq 2$  as long as certain values are avoided, or else for  $\lambda \geq 2.7$ .

## ACKNOWLEDGMENTS

The authors gratefully acknowledge support from *Österreichischer Forschungsfonds* under project No. P13062-TPH.

- <sup>1</sup>C. Caccamo, Phys. Rep. **274**, 1 (1996).
- <sup>2</sup>A. Parola and L. Reatto, Adv. Phys. **44**, 211 (1995).
- <sup>3</sup>A. Parola and L. Reatto, Phys. Rev. Lett. **53**, 2417 (1984).
- <sup>4</sup>A. Parola and L. Reatto, Phys. Rev. A **31**, 3309 (1985).
- <sup>5</sup>L. Reatto, Phys. Lett. **72A**, 120 (1979).
- <sup>6</sup>M. Tau, A. Parola, D. Pini, and L. Reatto, Phys. Rev. E **52**, 2644 (1995).
- <sup>7</sup>A. Parola, A. Meroni, and L. Reatto, Phys. Rev. Lett. **62**, 2981 (1989).
- <sup>8</sup>A. Meroni, A. Parola, and L. Reatto, Phys. Rev. A **42**, 6104 (1990).
- <sup>9</sup>A. Parola, J. Phys. C: Solid State Phys. **19**, 5071 (1986).
- <sup>10</sup>A. Parola and L. Reatto, Phys. Rev. A **44**, 6600 (1991).
- <sup>11</sup>D. Pini, A. Parola, and L. Reatto, J. Stat. Phys. **72**, 1179 (1993).
- <sup>12</sup>A. Parola, D. Pini, and L. Reatto, Phys. Rev. E **48**, 3321 (1993).
- <sup>13</sup>A. Meroni, L. Reatto, and M. Tau, Mol. Phys. **80**, 977 (1993).
- <sup>14</sup>F. Barocchi, P. Chieux, R. Fontana, R. Magli, A. Meroni, A. Parola, L. Reatto, and M. Tau, J. Phys.: Condens. Matter **9**, 8849 (1997).
- <sup>15</sup>M. J. P. Nijmeijer, A. Parola, and L. Reatto, Phys. Rev. E **57**, 465 (1998).
- <sup>16</sup>L. Reatto and A. Parola, J. Phys.: Condens. Matter **8**, 9221 (1996).
- <sup>17</sup>A. Parola and L. Reatto, J. Phys.: Condens. Matter **5**, B165 (1993).
- <sup>18</sup>D. Pini, A. Parola, and L. Reatto, J. Stat. Phys. **100**, 13 (2000).
- <sup>19</sup>A. Reiner and G. Kahl, Phys. Rev. E **65**, 046701 (2002); e-print cond-mat/0112035.
- <sup>20</sup>A. Reiner, Ph.D. thesis, Technische Universität Wien, 2002. Available on the world wide web from <http://purl.oclc.org/NET/a-reiner/dr-thesis/>
- <sup>21</sup>L. Vega, E. de Miguel, and L. F. Rull, J. Chem. Phys. **96**, 2296 (1992).
- <sup>22</sup>E. de Miguel, Phys. Rev. E **55**, 1347 (1997).
- <sup>23</sup>G. Orkoulas and A. Z. Panagiotopoulos, J. Chem. Phys. **110**, 1581 (1999).
- <sup>24</sup>N. V. Brilliantov and J. P. Valleau, J. Chem. Phys. **108**, 1115 (1998).
- <sup>25</sup>N. V. Brilliantov and J. P. Valleau, J. Chem. Phys. **108**, 1123 (1998).
- <sup>26</sup>J. R. Elliott and L. Hu, J. Chem. Phys. **110**, 3043 (1999).
- <sup>27</sup>A. Lomakin, N. Asherie, and G. B. Benedek, J. Chem. Phys. **104**, 1646 (1996).
- <sup>28</sup>D. M. Heyes and P. J. Aston, J. Chem. Phys. **97**, 5738 (1992).
- <sup>29</sup>J. Chang and St. I. Sandler, Mol. Phys. **81**, 745 (1994).
- <sup>30</sup>A. L. Benavides, J. Alejandre, and F. del Rio, Mol. Phys. **74**, 321 (1991).
- <sup>31</sup>G. Orkoulas, M. E. Fisher, and A. Z. Panagiotopoulos, Phys. Rev. E **63**, 051507 (2001).
- <sup>32</sup>J. A. White, J. Chem. Phys. **113**, 1580 (2000).
- <sup>33</sup>L. Lue and J. M. Prausnitz, J. Chem. Phys. **108**, 5529 (1998).
- <sup>34</sup>J. A. White and Sh. Zhang, J. Chem. Phys. **103**, 1922 (1995).
- <sup>35</sup>J. A. White and Sh. Zhang, J. Chem. Phys. **99**, 2012 (1993).
- <sup>36</sup>R. V. Gopala and D. Debnath, Colloid Polym. Sci. **268**, 604 (1990).
- <sup>37</sup>A. Lang, G. Kahl, Ch. N. Likos, H. Löwen, and M. Watzlawek, J. Phys.: Condens. Matter **11**, 10143 (1999).
- <sup>38</sup>G. Foffi, E. Zaccarelli, F. Sciortino, P. Tartaglia, and K. A. Dawson, J. Stat. Phys. **100**, 363 (2000).
- <sup>39</sup>L. Acedo and A. Santos, J. Chem. Phys. **115**, 2805 (2001).
- <sup>40</sup>E. Zaccarelli, G. Foffi, K. A. Dawson, F. Sciortino, and P. Tartaglia, Phys. Rev. E **63**, 031501 (2001).
- <sup>41</sup>M. E. Fisher and G. Orkoulas, Phys. Rev. Lett. **85**, 696 (2000).
- <sup>42</sup>G. Orkoulas, M. E. Fisher, and Cevat Üstün, J. Chem. Phys. **113**, 7530 (2000).
- <sup>43</sup>G. Stell, Phys. Rev. **184**, 135 (1969).
- <sup>44</sup>G. Stell, J. Chem. Phys. **55**, 1485 (1971).
- <sup>45</sup>H. C. Andersen and D. Chandler, J. Chem. Phys. **55**, 1497 (1971).
- <sup>46</sup>M. E. Fisher, J. Math. Phys. **5**, 944 (1964).
- <sup>47</sup>C. Caccamo, G. Pellicane, D. Costa, D. Pini, and G. Stell, Phys. Rev. E **60**, 5533 (1999).
- <sup>48</sup>K. G. Wilson, Phys. Rev. B **4**, 3184 (1971).
- <sup>49</sup>Available on the world wide web from <http://purl.oclc.org/NET/ar-hrt-1/>
- <sup>50</sup>H. Okumura and F. Yonezawa, J. Chem. Phys. **13**, 9162 (2000).
- <sup>51</sup>D. Pini, A. Parola, and L. Reatto, Mol. Phys. **100**, 1507 (2002); e-print cond-mat/0109311.